Rare Metal Materials and Engineering
Volume 50, Issue 7, July 2021
Available online at www.rmme.ac.cn

Science Press

Cite this article as: Wu Yanxia, Wang Xianzhong, Liang Hailong, et al. Effect of Potassium Salt Deposition on Denitration Performance of VMoTi Catalyst[J]. Rare Metal Materials and Engineering, 2021, 50(07): 2343-2351.

ARTICLE

Effect of Potassium Salt Deposition on Denitration Performance of VMoTi Catalyst

Wu Yanxia[1], Wang Xianzhong[2], Liang Hailong[1], Chen Xin[1], Chen Chen[1], Dai Changyou[3], Chen Yufeng[1]

[1] Ceramics Science Institute, China Building Materials Academy, Beijing 100024, China; [2] Jiangxi Key Laboratory of Industrial Ceramics, Pingxiang University, Pingxiang 337055, China; [3] Ruitai Materials Technology Co., Ltd, Beijing 100024, China

Abstract: VMoTi catalyst was prepared separately by impregnation method (IM) and sol-gel method, and the alkali metal K poisoning of the catalyst was simulated. The X-ray diffraction, BET specific surface area test, NH_3-temperature programmed desorption (TPD), H_2-temperature programmed reduction (TPR), and X-ray photoelectron spectroscopy (XPS) methods were used to analyze the physical and chemical properties of the VMoTi catalyst, and the reaction and deactivation mechanisms of the vanadium-titanium-based catalyst were discussed. The results show that compared with the catalyst prepared by IM, i.e., VMoTi (IM) catalyst, the catalyst prepared by the sol-gel method, i.e., VMoTi (Sol-gel) catalyst, has a smaller grain size, a larger specific surface area and pore volume, a larger amount of surface acid, a stronger redox capacity, and a higher content of V^{4+}, Mo^{4+}, and surface active oxygen. Therefore, VMoTi (Sol-gel) catalyst shows a good denitration efficiency stabilized at ~100% in the temperature range of 180~320 °C. The addition of potassium (alkali metal) leads to catalyst poisoning, and the poisoning effect of the catalysts prepared by different methods is different. The K salt deposition has a great influence on the denitration efficiency of the VMoTi (IM) catalyst. The VMoTi (Sol-gel) catalyst has good resistance to K poisoning. Through the characterization of the catalyst, it is found that K salt weakens the interaction between the active ingredient and the carrier, enhances the intensity of the diffraction peak of anatase TiO_2, and reduces the acidity and redox of the catalyst surface. At the same time, the content of chemical adsorption of oxygen and active metals, such as V^{4+} and Mo^{4+}, decreases. These factors are the main reasons of the catalyst inactivity.

Key words: catalyst; alkali metal; K poisoning; deactivation

Nitrogen oxides are one of the main atmospheric pollutants, which mainly cause environmental problems such as acid rain, photochemical smog, eutrophication of water bodies, greenhouse effect, and ozone layer destruction[1,2]. Due to the frequent occurrence of smog in recent years, the air pollution control attracts much attention. A series of NO_x emission standards have been formulated to strictly control the emission of nitrogen oxides. At present, the most mature fixed source denitration method is NH_3-selective catalytic reduction (SCR) denitration technique. Its main principle is to use NH_3 as a reducing agent to convert harmful nitrogen oxides in flue gas into harmless nitrogen and water through the action with catalyst[3,4].

Catalyst is an important part of SCR system, which accounts for more than 20% of the initial construction cost of SCR system. Its performance directly affects the overall denitration effect of SCR system. At present, the commercial VMoTi catalysts usually need to be replaced once every 1~2 years, so the catalyst life determines the operation cost of SCR system[5,6]. As coal is a complex natural substance, which contains many elements, such as Ca, K, Na, etc., the fly ash forming after combustion enters the SCR system and is adsorbed on the catalyst surface, thereby causing the alkali metal poisoning of catalyst and shortening the catalyst life[7,8]. The alkali metal potassium mainly exists in silicate minerals, and its content is generally higher than sodium content[9]. Studying the cause of catalyst alkali metal K poisoning and prolonging the service life of the catalyst are of great

Received date: July 16, 2020
Foundation item: National Natural Science Foundation of China (21866026)
Corresponding author: Wang Xianzhong, Ph. D., Professor, Jiangxi Key Laboratory of Industrial Ceramics, Pingxiang University, Pingxiang 337055, P. R. China, Tel: 0086-10-51167727, E-mail: fmud1972@163.com

Copyright © 2021, Northwest Institute for Nonferrous Metal Research. Published by Science Press. All rights reserved.

significance for reducing the operation cost of SCR system.

At present, the research on catalyst against alkali metal K poisoning mainly focuses on doping modification. Hu et al[10] found that the SiO_2-doped V_2O_5/TiO_2-SiO_2 catalyst is significantly better than V_2O_5/TiO_2 in potassium metal poisoning resistance. This is mainly due to the preferential combination of the potassium with the surface acid of V_2O_5/TiO_2-SiO_2, which reduces the toxicity of vanadium species. In addition, Nb-modified V_2O_5-Sb/TiO_2[11] and Sn-modified $CeSnO_x$[12] catalysts improve the poisoning resistance of alkali metal.

There are few studies about the influence of the preparation method on the poisoning resistance ability of catalyst. Previous studies showed that the preparation method affects the distribution of species on the catalyst surface, the type and number of surface active sites, the adsorption and activation of the reaction gas, and the catalyst performance. Therefore, the impregnation method (IM) and sol-gel method (Sol-gel) were used to prepare VMoTi catalyst and simulate the alkali metal K poisoning. The mechanism of the alkali metal K poisoning and the effect of the preparation method on the catalyst performance were investigated. X-ray diffraction (XRD), BET specific surface area test, NH_3-temperature programmed desorption (TPD), H_2-temperature programmed reduction (TPR) and X-ray photoelectron spectroscopy (XPS) methods were used to characterize the catalyst.

1 Experiment

A certain amount of ammonia metavanadate was dissolved in hot water. A small amount of monoethanolamine was added in the solution and stirred to dissolve. Then the ammonium heptamolybdate with a certain quantity was added and stirred until the solution was transparent. The precursor solution of vanadium molybdenum compound was prepared. A certain amount of TiO_2 powder was added into the vanadium molybdenum precursor solution. Then it was aged at room temperature and dried in air at 80 °C. Finally, it was calcined in muffle furnace at 500 °C for 4 h. The calcined catalyst was labeled as VMoTi (IM) catalyst, containing 3wt% V_2O_5/TiO_2 and 6wt% MoO_3/TiO_2 (Fig.1).

Liquid A was prepared by mixing 90 mL butyl titanate and 240 mL absolute ethanol. The 25 mL glacial acetic acid, 90 mL deionized water, and 240 mL absolute ethanol were mixed as liquid B. Ammonium metavanadate and ammonium heptamolybdate were added to liquid B to obtain liquid C. A mixed homogeneous sol was obtained by the slow addition of liquid A into liquid C after stirring for 20~30 min, then dried at 105 °C for 8 h, and finally calcined at 500 °C for 4 h. The calcined catalysts were labeled as VMoTi (Sol-gel) catalyst, containing 3wt% V_2O_5/TiO_2 and 6wt% MoO_3/TiO_2 (Fig.2).

The alkali metal K poisoning catalyst was prepared by the impregnation method. The K_2SO_4 solution was prepared according to the molar ratio of K element/V element of 2. The fresh catalysts prepared by sol-gel and impregnation methods were separately immersed in the K_2SO_4 solution for 5 h, then dried at 105 °C for 8 h, and finally calcined at 500 °C for 4 h. The calcined catalysts were labeled as K-VMoTi (IM) and K-VMoTi (Sol-gel), respectively (Fig.3).

A D8 advance X-ray diffractometer produced by German Bruker was used to characterize the catalysts. The test conditions were: current of 40 mA, voltage of 40 kV, Kα as the radiation source, Cu as the target, scanning range 2θ=10°~80°, step size of 0.02°.

The N_2 physical adsorption test of the catalyst was carried out by the Autosorb-iQ physical adsorption instrument to analyze the specific surface area and pore structure characteristics of the catalyst. First, a sample of 0.25~0.3 g was heated and evacuated at 240 °C for 2 h, and then tested

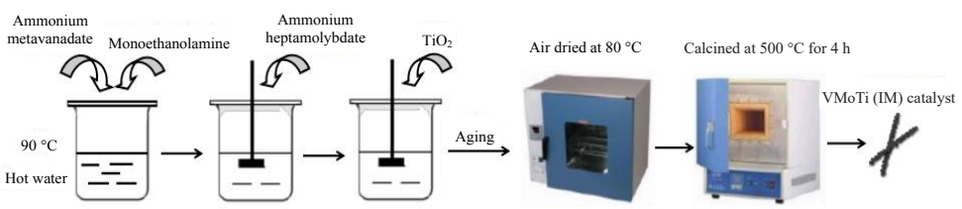

Fig.1 Synthesis procedure of VMoTi (IM) catalyst

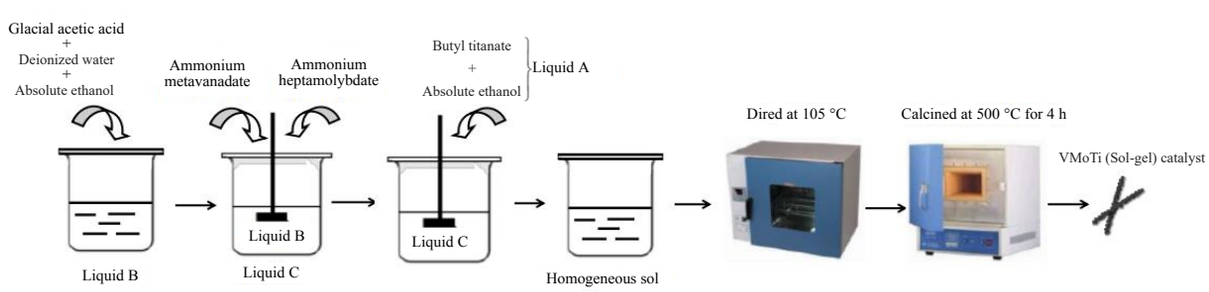

Fig.2 Synthesis procedure of VMoTi (Sol-gel) catalyst

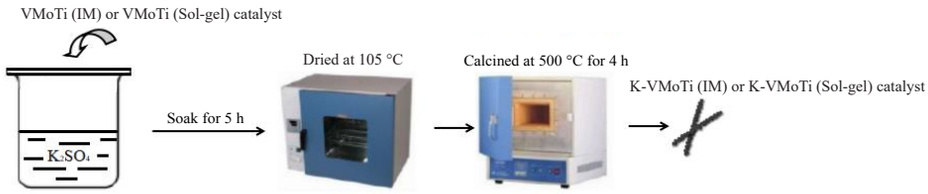

Fig.3 Synthesis procedure of K poisoned catalysts

under the condition of liquid nitrogen (-196 °C). The specific surface area was calculated using the multi-point BET equation, and the pore size and pore volume were measured using the BJH method.

The H_2-TPR characterization of the catalyst was carried out by the Auto Chem II 2920 type chemical adsorption instrument of Mike Corporation. The sample (mass of 50 mg, particle size of 0.3~0.45 mm) was pretreated at 300 °C for 0.5 h in the pure Ar atmosphere, and then cooled to 50 °C. Under the condition of 10vol% H_2/Ar (20 mL/min), the temperature was programmed to 900 °C at a rate of 10 °C/min. The H_2 consumption during this process was also detected by the thermal conductivity detector (TCD).

The NH_3-TPD characterization of the catalyst was carried out by the Auto Chem II 2920 type chemical adsorption instrument of Mike Corporation. The sample (mass of 100 mg, particle size of 0.3~0.45 mm) was pretreated at 400 °C for 0.5 h in the pure He atmosphere (20 mL/min), and then cooled to 50 °C. Next, the sample was fed with 5vol% NH_3/N_2 (20 mL/min) for 0.5 h for NH_3 adsorption, then the container was purged under the pure He atmosphere for 1 h, and finally the temperature was programmed to 550 °C at a rate of 10 °C/min. The attached NH_3 was detected by TCD.

The Thermo Scientific ESCALAB 250Xi X-ray photoelectron spectrometer was used for XPS characterization of the catalyst. The vacuum degree of the analysis chamber was 8×10^{-10} Pa, the excitation source was Al Kα ray ($h\nu$=1253.6 eV), the working voltage was 12.5 kV, the filament current was 16 mA, and the signal accumulation of 10 cycles was performed.

The activity evaluation of the catalyst was carried out in a stainless steel SCR fixed reactor. The temperature was controlled by the external heating of the tube furnace. The inside of the tube furnace was a stainless steel tube where the catalyst was placed. The stainless steel mesh prevented the catalyst from leaking. The schematic diagram of the specific experimental device is shown in Fig. 4. The standard steel cylinder gas was used to simulate flue gas, and the mass flow meter was used to control the flow. The composition of the simulated flue gas is as follows: 0.05vol% NO, 0.05vol% NH_3, 6vol% O_2, and abundant N_2 for the equilibrium carrier gas. The catalyst was in the form of granules with 40#~60#, and the accumulation volume was 12 mL, which was measured by a measuring cylinder. The total gas flow rate was 1000 mL/min, and the space velocity was 5000 h^{-1}. The activity was evaluated at 80~380 °C. The German Testo 350 flue gas analyzer was used to detect the NO concentration before and after the reaction, and the NO removal rate was calculated according to Eq.(1) as follows:

$$\eta=\frac{V_{\text{NO-in}}-V_{\text{NO-out}}}{V_{\text{NO-in}}} \quad (1)$$

where $V_{\text{NO-in}}$ and $V_{\text{NO-out}}$ are the volume of NO gas input and output, respectively, mg/m^3.

2 Results and Discussion

2.1 Denitration efficiency of different catalysts

It can be seen from Fig.5 that the denitration efficiency (NO conversion ratio) of fresh catalysts shows an increasing trend at first, then remains stable, and finally decreases with increasing the temperature. VMoTi (IM) catalyst has a stable denitration efficiency of nearly 100% in the temperature range of 200~280 °C. The temperature range of the VMoTi (Sol-gel) catalyst is wider than that of VMoTi (IM) catalyst, as the initial and terminal temperatures of the temperature range migrate slightly to the low and high temperatures, respectively. In the temperature range of 180~320 °C, the denitration efficiency is stable at nearly 100%, indicating that

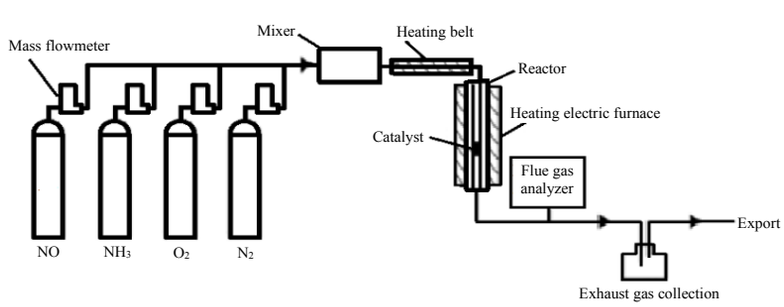

Fig.4 Schematic diagram of activity evaluation device for catalyst

the sol-gel method widens the temperature window of the catalyst. When the temperature is higher than 300 °C, the denitrification efficiency of fresh catalysts begins to decrease, which is mainly due to the catalytic oxidation of NH_3 to NO_x at higher temperature. Therefore, the conversion of NO of VMoTi (Sol-gel) catalyst is higher than 90% at 160 °C, and close to 100% at 180~320 °C. It can also be seen from Fig. 5 that after the alkali metal K is added, the denitration efficiency of the catalyst significantly reduces, and the denitration efficiency of K-VMoTi (Sol-gel) catalyst is generally higher than that of K-VMoTi (IM) catalyst. It can be concluded that alkali metal K poisons the VMoTi (IM) and VMoTi (Sol-gel) catalysts, and the poison resistance of alkali metal K of VMoTi (Sol-gel) catalyst significantly improves.

2.2 N_2 selectivity of different catalysts

NH_3-SCR reaction produces new nitrogen oxides, which causes environmental pollution. Therefore, the N_2 selectivity of the catalyst is one of the key issues in the development of new catalysts. The change in N_2 selectivity of the catalyst with temperature is shown in Fig. 6. It can be seen from Fig. 6 that the N_2 selectivity of each catalyst decreases with the increase of reaction temperature, suggesting the excellent N_2 selectivity at medium and low temperatures. When the temperature is higher than 250 °C, the N_2 selectivity begins to decrease gradually due to the occurrence of side reactions caused by high temperature and the formation of N_2O. It should be noted that the N_2 selectivity of the catalysts decreases after K poisoning. At 360 °C, the N_2 selectivity of the K-VMoTi (Sol-gel) catalyst remains above 85%, while that of K-VMoTi (IM) catalyst is ~75%.

2.3 XRD analysis of different catalysts

It can be seen from Fig. 7 that the diffraction peaks of the catalysts before and after K poisoning are mainly anatase titanium dioxide peaks[13,14], and there are no diffraction peaks of V_2O_5 and MoO_3. The reason may be that the content of V_2O_5 and MoO_3 in the catalyst is too low, and V_2O_5 and MoO_3 are still distributed on the carrier in high dispersion or indefinite form. The TiO_2 characteristic peak of VMoTi (IM) catalyst is sharp, and the peak is narrow, which indicates that the crystallization performance is good, and the grain size

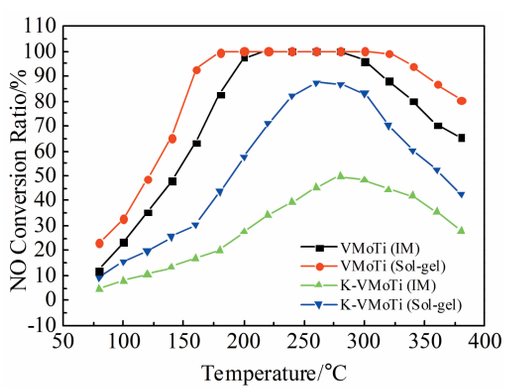

Fig.5 NO conversion ratio of different catalysts

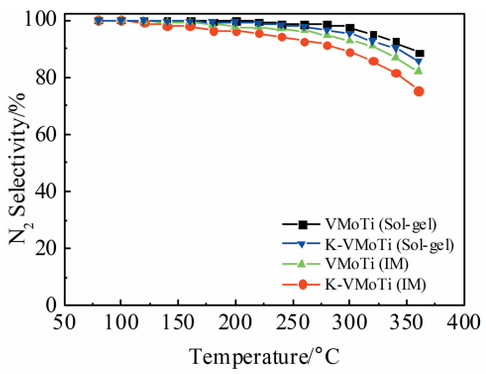

Fig.6 N_2 selectivity of different catalysts

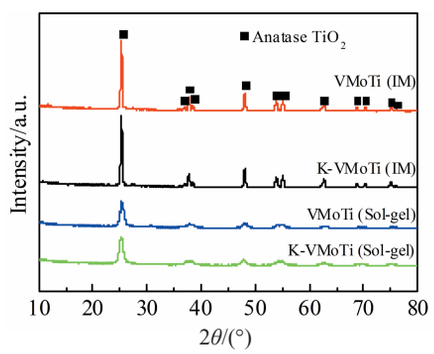

Fig.7 XRD patterns of different catalysts

increases. The VMoTi (Sol-gel) catalyst has low diffraction peak intensity, and the TiO_2 peak is obviously wider than that of VMoTi (IM) catalyst. The reason may be that the grain size is small and the surface effect tends to be obvious, which leads to the decrease of the order degree, the poor crystallinity, and the appearance of a certain amount of amorphous components[15]. The poisoning of the catalyst does not affect the distribution of the original components of the catalyst. However, the anatase TiO_2 characteristic peak intensity of the poisoned K-VMoTi (IM) and K-VMoTi (Sol-gel) catalysts is stronger than that of the VMoTi (IM) and VMoTi (Sol-gel) catalysts, indicating that the addition of alkali metal weakens the interaction between the active components and the support[16].

2.4 BET analysis of different catalysts

The BET analysis results of the catalysts are listed in Table 1. It can be seen from Table 1 that the specific surface area

Table 1 BET analysis results of different catalysts

Sample	A_{BET}/ $m^2 \cdot g^{-1}$	Pore volume/ $cm^3 \cdot g^{-1}$	Pore size/ nm
VMoTi (IM)	58.8	0.11	8.21
K-VMoTi (IM)	56.7	0.10	8.23
VMoTi (Sol-gel)	63.4	0.12	8.12
K-VMoTi (Sol-gel)	61.6	0.11	8.14

(A_{BET}) of the VMoTi (IM) catalyst is 58.8 $m^2 \cdot g^{-1}$, the average pore volume is 0.11 $cm^3 \cdot g^{-1}$, and the average pore size is 8.21 nm. The specific surface area of the VMoTi (Sol-gel) catalyst is 63.4 $m^2 \cdot g^{-1}$, the average pore volume is 0.12 $cm^3 \cdot g^{-1}$, and the average pore size is 8.12 nm. Compared with the properties of VMoTi (IM) catalyst, the specific surface area and average pore volume of the VMoTi (Sol-gel) catalyst increase and the average pore size decreases. The result shows that the NH_3-SCR reaction takes place at the catalyst surface. A larger specific surface area is conducive to the high dispersion of active components, which provides more active sites, absorbs more reaction gases, and promotes the NH_3-SCR catalytic reaction[17-19]. Compared with the properties of fresh catalysts, the deposition of the alkali metal salt particles on the surface and the blockage of some pores of the deactivated catalyst cause slight changes: the specific surface area and the total pore volume slightly reduces, and the average pore size slightly increases.

Fig. 8 shows the N_2 adsorption-desorption curves of different catalysts. It can be seen from Fig.8 that VMoTi (IM) and K-VMoTi (IM) catalysts are Langmuir IV isotherms with H_3 hysteresis loops, which indicates that both catalysts have the mesoporous structure. There is no obvious saturated adsorption platform in the hysteresis isotherm, which indicates that the pore structure of the catalysts is very incomplete, mainly including plate slit structure, crack structure, and wedge structure[20,21]. However, both the VMoTi (Sol-gel) and K-VMoTi (Sol-gel) catalysts have Langmuir IV isotherms and H_4 hysteresis loops, which shows a mixture of micro-porous and mesoporous materials[22,23]. After K poisoning, the hysteresis loop of the catalysts becomes smaller, which indicates that the residence time of reaction gas on the surface of poisoned catalyst becomes shorter, and the reaction gas is easy to desorb, which is not conducive to the full progress of SCR reaction. Therefore, the low-temperature activity of the catalyst decreases after K poisoning. Fig.9 shows the pore size distribution of different catalysts. It can be seen from Fig. 9 that the pore size of VMoTi (IM) catalyst is 0~5 nm, while the

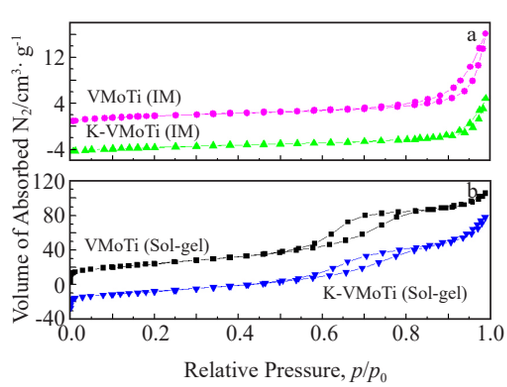

Fig.8 Adsorption-desorption curves of VMoTi (IM) and K-VMoTi (IM) catalysts (a) and VMoTi (Sol-gel) and K-VMoTi (Sol-gel) catalysts (b)

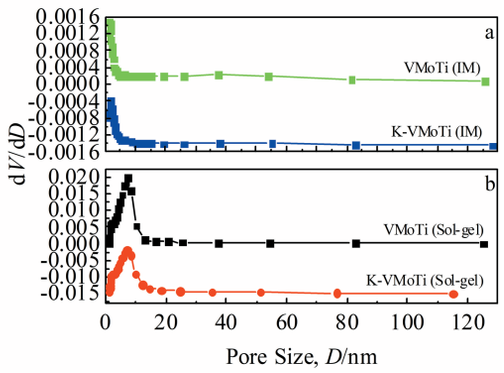

Fig.9 Pore size distribution of VMoTi (IM) and K-VMoTi (IM) catalysts (a) and VMoTi (Sol-gel) and K-VMoTi (Sol-gel) catalysts (b)

pore size of 5~10 nm in VMoTi (Sol-gel) catalyst significantly increases. Compared with the properties of catalyst before poisoning, the number of pores in K-VMoTi (IM) and K-VMoTi (Sol-gel) catalysts decreases significantly after K poisoning. In the mesoporous range, proper increase of the pore radius of the catalyst is conducive to the adsorption and desorption of reaction gas molecules at the active sites on the catalyst surface, resulting in better catalytic reaction[18].

2.5 NH_3-TPD analysis of different catalysts

According to Eley-Rideal mechanism, NH_3 is firstly adsorbed at the active acid site of catalyst, and then reacts with NO under gaseous or weak adsorption state. The adsorption of NH_3 at the active site is a control step of SCR catalytic reaction[15]. According to the literatures[24,25], in the NH_3-TPD spectrum, Lewis acid site is mainly located in the range above 350 °C, while Brønsted acid site is mainly located in the range below 350 °C. Moreover, many researchers have found that SCR activity is directly proportional to the number of Brønsted acid sites, but not significantly related to the number of Lewis acid sites.

It can be seen from Fig. 10 that VMoTi (IM) and VMoTi (Sol-gel) catalysts have a weak broad adsorption peak

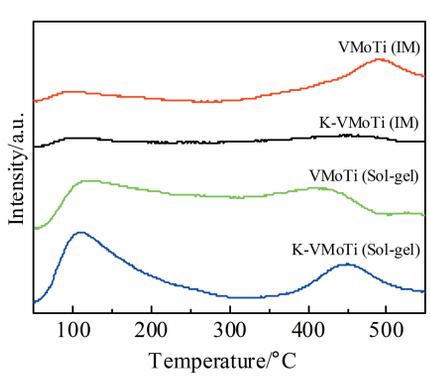

Fig.10 NH_3-TPD spectra of different catalysts

between 100~200 °C caused by the adsorption of NH_3 at the weak acid site (Brønsted acid site) on the catalyst surface, and an adsorption peak between 400~500 °C caused by the adsorption of NH_3 at the medium strength acid site (Lewis acid site) on the catalyst surface. The amount of acid on the surface of VMoTi (Sol-gel) catalyst increases by 2~3 times compared with that of VMoTi (IM) catalyst. It can be seen that the preparation method has a very obvious effect on the Brønsted acid site. By comparing the NH_3-TPD results of the catalyst before and after poisoning, it is found that the weak adsorption peak at low temperature and the Lewis acidic site adsorption peak between 400~500 °C are all weakened after K deposition. According to SCR reaction mechanism, it is generally believed that NH_3 is firstly adsorbed on the catalyst surface, and then undergoes a redox reaction with the adsorbed NO. The acidity of catalyst surface is an important factor affecting the adsorption capacity of NH_3. Potassium poisoning reduces the acid capacity of catalyst surface, which is one of the main factors for the decrease of SCR activity[26,27]. The acid amount of K-VMoTi (IM) catalyst decreases more than that of K-VMoTi (Sol-gel) catalyst does.

2.6 H_2-TPR analysis of different catalysts

During the process of catalytic reaction, the catalyst, as the reaction medium, accelerates the transmission of electrons, promotes the formation of activated molecules, thus reduces the activation energy required for the reaction, and improves the speed of the reaction towards thermodynamic equilibrium. The ability of the catalyst to gain and lose electrons corresponds to the redox ability of the catalyst. The commonly used technique for characterizing the redox performance of catalysts is H_2-TPR[28] technique.

Fig. 11 is the H_2-TPR spectra of different catalysts. According to the literature[29], MoO_3 undergoes a reduction reaction of $Mo^{6+}\rightarrow Mo^{4+}\rightarrow Mo$ at 400~800 °C, and $V^{5+}\rightarrow V^{4+}\rightarrow V^{3+}\rightarrow V^{2+}$ reduction process occurs at 500~800 °C for dispersed V_2O_5 and poly-vanadium oxygen species. The peak near 650 °C belongs to the hydrogen consumption peak of the hydroxyl group on the TiO_2 surface. It can be seen that the peaks appearing near 500 °C in Fig.11 belong to the overlapping peaks of the reduction of vanadium species and molybdenum species. The peaks around 700~800 °C belong to the reduction peak of TiO_2. The reduction peak position of VMoTi (Sol-gel) catalyst moves to the low temperature region because molybdenum species play an important role in storing/releasing oxygen and promoting the reduction of V_2O_5. Organic impurities decrease, thereby reducing the reduction temperature of TiO_2. The reducibility of the catalyst is determined by the grain arrangement and grain structure. The interaction between the alkali metal K and the composite oxide makes the crystal arrangement irregular. The poor alignment makes the catalyst exhibit poor reducibility, which causes the peak temperature to shift toward the high temperature region[30]. The migration of reduction peak temperature towards high temperature and the reduction of peak area indicate that the activity of oxygen species on the catalyst surface significantly reduces after alkali metal K poisoning, VO_x and MoO_x species are difficult to reduce, and the redox performance of catalyst metal reduces, thus affecting the SCR reaction process (such as NH_3 activation and NO oxidation).

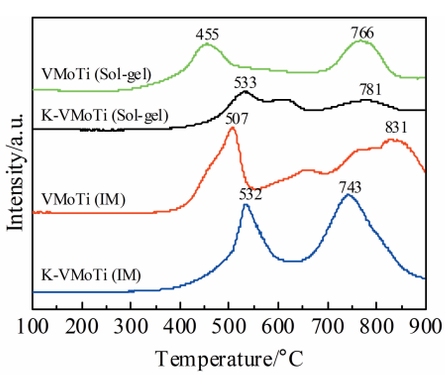

Fig.11 H_2-TPR spectra of different catalysts

2.7 XPS analysis of different catalysts

The electronic energy spectra of the O 1s orbit of the catalysts are shown in Fig. 12a. The oxygen with binding energy between 530.1~530.3 eV is lattice oxygen (O^{2-}, labeled as O_{latt}), and the oxygen between 531.4~531.7 eV is surface adsorbed oxygen (O^- and O_2^{2-}, labeled as O_{ads})[31,32]. It has been reported that chemisorption of oxygen on the surface is the most active type of oxygen. Due to its high mobility, it plays an important role in the oxidation reaction. High O_{ads} content produces strong oxidation capacity, which is conducive to the oxidation of NO to NO_2, and promotes the rapid SCR reaction[33]. According to the results in Table 2, the value of $O_{ads}/(O_{latt}+O_{ads})\times100\%$ of VMoTi (IM) and VMoTi (Sol-gel) catalysts is 21.08% and 41.37%, respectively. The proportion of chemically adsorbed oxygen on the surface of the catalyst affects the progress of the redox reaction to a certain extent, and plays a role in the denitration activity of the catalyst together with other factors, such as surface acid sites and redox properties. After alkali metal K poisoning, the adsorbed oxygen concentration $O_{ads}/(O_{latt}+O_{ads})\times100\%$ on the surface of K-VMoTi (IM) and K-VMoTi (Sol-gel) catalysts decreases to 16.91% and 24.25%, respectively. This is due to the introduction of K_2O and oxygen to compete for oxygen vacancy on the catalyst surface. K_2O and oxygen vacancy on the catalyst surface form a strong adsorption, reducing the peak of adsorbed oxygen[34]. Therefore, the decrease in ratio of chemisorption oxygen is another factor for the activity decrease of the K-poisoned catalyst.

The electron energy spectra of the V 2p orbit of the catalyst are shown in Fig. 12b. The vanadium with a binding energy between 516.5~516.7 eV exists in the form of V^{4+}, and the vanadium between 517.4~517.6 eV exists in the form of V^{5+}. It can be seen from Table 2 that the values of $V^{4+}/(V^{4+}+V^{5+})\times100\%$ of VMoTi (IM) and VMoTi (Sol-gel) catalysts are similar, which are 49.00% and 48.20%, respectively. After alkali metal K poisoning, the value of $V^{4+}/(V^{4+}+V^{5+})\times100\%$ of K-VMoTi (IM) and K-VMoTi (Sol-gel) catalysts decreases to

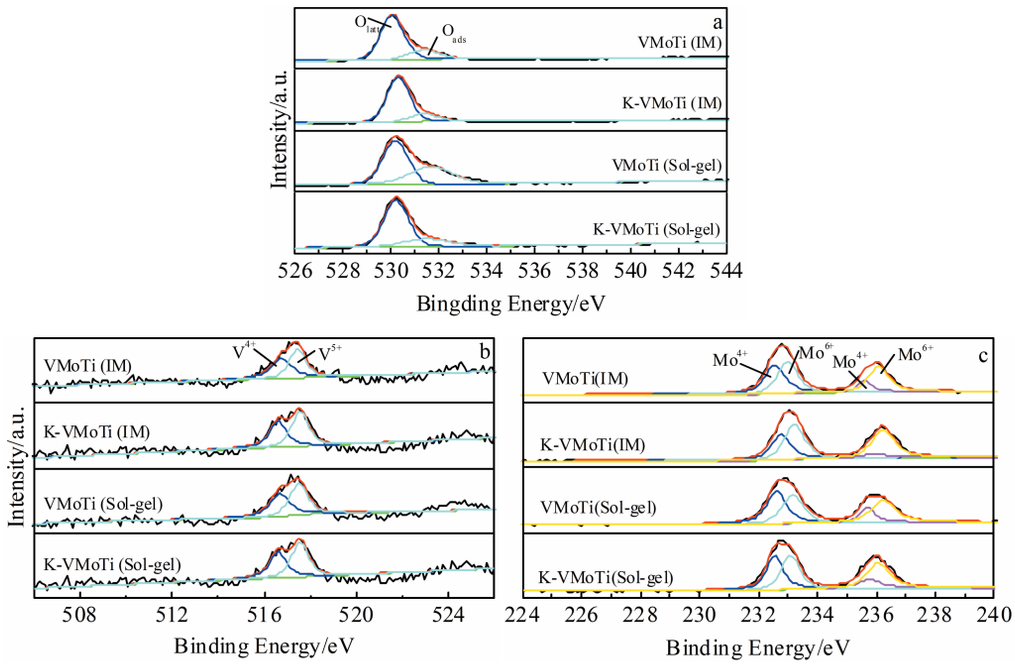

Fig.12 XPS spectra of different orbits of catalysts: (a) O 1s, (b) V 2p, and (c) Mo 3d

Table 2 Binding energy and surface atomic concentration of different catalysts

Sample			VMoTi (IM)	K-VMoTi (IM)	VMoTi (Sol-gel)	K-VMoTi (Sol-gel)
Binding energy of O 1s/eV	O_{latt}		530.1	530.3	530.2	530.2
	O_{ads}		531.4	531.4	531.7	531.5
Binding energy of V 2p/eV	V^{4+}		516.7	516.6	516.7	516.5
	V^{5+}		517.4	517.6	517.5	517.4
Binding energy of Mo 3d/eV	$3d_{5/2}$	Mo^{4+}	232.6	232.8	232.6	232.6
		Mo^{6+}	233	233.2	233.2	233.1
	$3d_{3/2}$	Mo^{4+}	235.6	235.9	235.7	235.7
		Mo^{6+}	236.1	236.2	236.2	236.1
Value of $O_{ads}/(O_{ads}+O_{latt})$/%			21.08	16.91	41.37	24.25
Value of $V^{4+}/(V^{4+}+V^{5+})$/%			49.00	45.00	48.20	47.24
Value of $Mo^{4+}/(Mo^{4+}+Mo^{6+})$/%			41.22	32.52	45.40	41.95

45.00% and 47.24%, respectively. The value of $V^{4+}/(V^{4+}+V^{5+})\times 100\%$ has an important effect on the denitration activity of the catalyst. The presence of non-stoichiometric vanadium species (V^{n+}, $n\leqslant 4$) is conducive to the electron transfer. Within a certain range, the value of $V^{4+}/(V^{4+}+V^{5+})\times 100\%$ is positively correlated with the denitration activity of the catalyst[35]. The increase of metastable V^{4+} ions enhances the reduction degree of vanadium species. The electron transfer between ions of different valences provides power for the SCR reaction. In SCR reaction, V^{4+} and V^{5+} on the surface of catalyst mainly exist in the form of V-OH and V=O. NO in flue gas is oxidized to NO_2, and V^{5+}=O is reduced to V^{4+}-OH, which promotes the "fast SCR" reaction and improves the low temperature activity of catalyst[36].

The electron energy spectra of the Mo 3d orbit of the catalyst are shown in Fig. 12c. There are 4 different characteristic peaks in the Mo fitting peaks of the catalysts. Among them, the peak binding energy of 232.6~232.8, 233.0~233.2, 235.6~235.9, and 236.1~236.2 eV belongs to Mo^{4+} species in Mo $3d_{5/2}$ orbit, Mo^{6+} species in Mo $3d_{5/2}$ orbit, Mo^{4+} species in Mo $3d_{3/2}$ orbit, and Mo^{6+} species in Mo $3d_{3/2}$ orbit, respectively. Mo mainly exists in the form of Mo^{4+} and Mo^{6+} [37,38]. The value of $Mo^{4+}/(Mo^{4+}+Mo^{6+})\times 100\%$ of the VMoTi (IM) and VMoTi (Sol-gel) catalysts is 41.22% and 45.40%, respectively. This is mainly because MoO_x and VO_x of the VMoTi (Sol-gel) catalyst have a good interaction. More Mo^{6+} is reduced to Mo^{4+}, which enhances the reduction degree of Mo. At the same time, the formation of oxygen defects due to the unbalanced charge is conducive to the improvement of catalyst activity[39]. After alkali metal K poisoning, the value of $Mo^{4+}/(Mo^{4+}+Mo^{6+})\times 100\%$ of K-VMoTi (IM) and K-VMoTi (Sol-gel) catalysts drops to 32.52% and 41.95%, respectively.

Therefore, the VMoTi (Sol-gel) catalyst has more surface acidity, stronger redox ability, and more V^{4+}, Mo^{4+}, and surface reactive oxygen species. Besides, the VMoTi (Sol-gel) catalyst shows better resistance to K-metal poisoning. The mechanism of K poisoning is that the K salt weakens the interaction between active component and support, enhances the intensity of diffraction peak of anatase TiO_2, reduces the surface acidity and redox property of the catalyst, and reduces the chemically adsorbed oxygen and the active metal contents, such as V^{4+} and Mo^{4+}, on the catalyst surface.

2.8 Denitrification mechanism

According to the Lewis acid mechanism, the SCR reaction process is as follows:

$$NH_3+M^{n+}+O^{2-}\rightarrow M^{(n-1)+}\cdots NH_2+OH^- \quad (2)$$

$$M^{(n-1)+}\cdots NH_2+NO\rightarrow M^{(n-1)+}\cdots NH_2NO \quad (3)$$

$$M^{(n-1)+}\cdots NH_2NO\rightarrow M^{(n-1)}+N_2+H_2O \quad (4)$$

$$2M^{(n-1)+}+1/2O_2\rightarrow 2M^{n+}+O^{2-} \quad (5)$$

$$2OH^-\rightarrow H_2O+O^{2-} \quad (6)$$

In V_2O_5-$WO_3(MoO_3)/TiO_2$ system, the active center M^{n+} is V^{5+}. The mechanism shows that NH_3 adsorbed on Lewis acid site is activated to dehydrogenate to form NH_2 through the action of lattice oxygen or surface oxygen. At the same time, the adsorption site is reduced from V^{5+} to V^{4+}, and the intermediate $V^{4+}\cdots NH_2$ forms. Then the intermediate $V^{4+}\cdots NH_2$ and NO form $V^{4+}\cdots NH_2NO$, which decomposes into N_2 and H_2O, and the reduced adsorption site V^{4+} is oxidized to V^{5+} under the action of O_2. It can be seen from the reaction process that the formation of $NH_3\rightarrow NH_2$ (adsorbed) intermediate is a key step in the whole reaction process[40].

According to the results, it is observed that K_2O occupies the oxygen vacancy on the catalyst surface, reduces the amount of surface oxygen, inhibits the formation of NH_2 (adsorbed) in Eq.(2), and indirectly inhibits the reoxidation of adsorption site in Eq.(5)[41]. In addition, the valence state of V on the catalyst surface also has influence on its catalytic performance. It is speculated that the introduction of K changes the surface properties of catalyst. K reacts with V-OH on the catalyst surface to form V-O-K, which changes the chemical environment of metal oxides, such as V_2O_5 and MoO_3. Compared with the fresh catalyst, the value of $V^{4+}/(V^{4+}+V^{5+})\times100\%$ in the deactivated catalyst decreases significantly, which inhibits the formation of NH_2 (adsorbed). Therefore, the catalyst surface activity not only is related to the acid sites and the content of chemically adsorbed oxygen on the surface, but also has a certain positive correlation with the morphology of V on the surface-active center and the value of $V^{4+}/(V^{4+}+V^{5+})\times100\%$.

3 Conclusions

1) Compared with the catalysts prepared by the impregnation method, i. e., VMoTi (IM) catalyst, the catalyst prepared by sol-gel method, i.e., VMoTi (Sol-gel) catalyst, has smaller grain size, larger specific surface area and pore volume, more surface acidity, stronger redox ability, and more V^{4+}, Mo^{4+}, and surface reactive oxygen species. Therefore, the VMoTi (Sol-gel) catalyst shows good denitrification efficiency, and the conversion ratio of NO is close to 100% at 180~320 °C.

2) Potassium salt leads to alkali metal poisoning and reduces the denitration activity of catalyst. The VMoTi (Sol-gel) catalyst shows better resistance to K-metal poisoning. The main reason of K poisoning is that the K salt weakens the interaction between active component and support, enhances the intensity of diffraction peak of anatase TiO_2, reduces the surface acidity and redox property of the catalyst, and reduces the chemically adsorbed oxygen and the active metal contents, such as V^{4+} and Mo^{4+}, on the catalyst surface.

References

1 Busca G, Lietti L, Ramis G *et al*. *Applied Catalysis B: Environmental*[J], 1998, 18(1-2): 1

2 Zhu Sheming, Li Weifeng, Chen Yingwen *et al*. *Environmental Pollution & Control*[J], 2005, 27(9): 699 (in Chinese)

3 Zhang Daojun, Ma Ziran, Sun Qi *et al*. *Chemical Industry and Engineering Progress*[J], 2019, 38(4): 1611 (in Chinese)

4 Huang Haifeng, Zeng Li, Lu Hanfeng *et al*. *Journal of Chemical Engineering of Chinese Universities*[J], 2009, 23(5): 871 (in Chinese)

5 Zhang Yaping, Guo Wanqiu, Wang Longfei *et al*. *Chinese Journal of Catalysis*[J], 2015, 36(10): 1701

6 Huang Yan, Meng Qinghua, Jin Qian *et al*. *Industrial Catalysis* [J], 2015, 23(4): 301 (in Chinese)

7 Kong Ming, Liu Qingcai, Jiang Lijun *et al*. *Chemical Engineering Journal*[J], 2019, 370: 518

8 Liu Zhiming, Zhang Shaoxuan, Li Junhua *et al*. *Applied Catalysis B: Environmental*[J], 2014, 158-159: 11

9 Zhou Xuerong, Zhang Xiaopeng. *Chemistry*[J], 2015, 78(7): 590 (in Chinese)

10 Hu Shilei, Ye Daiqi, Fu Mingli. *Chinese Journal of Inorganic Chemistry*[J], 2008, 24(7): 1113 (in Chinese)

11 Haheon P, Chungsoon H, Ohyoung J. *Rare Metals*[J], 2006, 25(S2): 84

12 Li Xiaoliang, Li Yonghong, Deng Shanshan *et al*. *Catalysis Communications*[J], 2013, 40: 47

13 Chen Jinfeng, Zhang Xiaodong, Shi Xiaoyu *et al*. *Journal of Colloid and Interface Science*[J], 2020, 579: 37

14 Chen Jinfeng, Zhang Xiaodong, Bi Fukun *et al*. *Journal of Colloid and Interface Science*[J], 2020, 571: 275

15 Shen Boxiong, Ma Juan. *Journal of Fuel Chemistry and Technology*[J], 2012, 40(2): 247 (in Chinese)

16 Li Hongyan, Zhu Zhiliang, Yang Fengli *et al*. *Journal of the Chinese Ceramic Society*[J], 2012, 40(4): 577 (in Chinese)

17 Wang Liangliang, Wang Minghong, Fei Zhaoyang *et al*. *Journal of Fuel Chemistry and Technology*[J], 2017, 45(8): 993 (in Chinese)

18 Tang Nan, Huang Yan, Li Yuanyuan *et al*. *Journal of Molecular Catalysis*[J], 2018, 32(3): 240 (in Chinese)

19 Fu Yincheng, Song Hao, Wu Weihong *et al*. *Energy Engineering* [J], 2011(2): 40 (in Chinese)
20 Yan Dongjie, Yu Ya, Huang Xuemin *et al*. *Journal of Fuel Chemistry and Technology*[J], 2016, 44(2): 232 (in Chinese)
21 Bi Fukun, Zhang Xiaodong, Xiang Shang *et al*. *Journal of Colloid and Interface Science*[J], 2020, 573: 11
22 Ma Tengkun, Fang Jingrui, Sun Yong *et al*. *Journal of Fuel Chemistry and Technology*[J], 2017, 45(4): 491 (in Chinese)
23 Bi Fukun, Zhang Xiaodong, Chen Jinfeng *et al*. *Applied Catalysis B: Environmental*[J], 2020, 269: 118 767
24 Du Zhen, Fu Yincheng, Qian Xuyue *et al*. *Thermal Power Generation*[J], 2014, 43(7): 72 (in Chinese)
25 Zheng Li, Zhou Meijuan, Huang Zhiwei *et al*. *Environmental Science & Technology*[J], 2016, 50(21): 11 951
26 Wu Yanxia, Liang Hailong, Zhao Chunlin *et al*. *Petroleum Processing and Petrochemicals*[J], 2019, 50(4): 44 (in Chinese)
27 Zhu Shaowen, Shen Boxiong, Chi Guilong *et al*. *Chinese Journal of Environmental Engineering*[J], 2017, 11(6): 3633 (in Chinese)
28 Li Hao. *Thesis for Master*[D]. Jinan: University of Jinan, 2016 (in Chinese)
29 Li Zeying, Tang Qing, Zuo Zhaohong *et al*. *Industrial Catalysis* [J], 2016, 24(7): 41
30 Wang Junjie, Zhang Yaping, Wang Wenxuan *et al*. *Journal of Fuel Chemistry and Technology*[J], 2016, 44(7): 888
31 Wang Yin, Yu Lan, Wang Ruotong *et al*. *Journal of Colloid and Interface Science*[J], 2020, 574: 74
32 Zhang Xiaodong, Lv Xutian, Bi Fukun *et al*. *Molecular Catalysis* [J], 2020, 482: 110 701
33 Sun Hui. *Thesis for Master*[D]. Harbin: Harbin Engineering University, 2017 (in Chinese)
34 Fang De, He Feng, Li Fengxiang *et al*. *Journal of Wuhan University of Technology*[J], 2017, 39(12): 7
35 Lin Zhuowei. *Thesis for Master*[D]. Beijing: North China Electric Power University, 2017 (in Chinese)
36 Jia Yong, Zhang Song, Dai Bo *et al*. *Chinese Journal of Environmental Engineering*[J], 2019, 13(1): 125 (in Chinese)
37 Wang Penglu, Wang Haiqiang, Chen Xiongbo *et al*. *Chem Cat Chem*[J], 2016, 8(4): 787
38 Peng Yue, Li Junhua, Shi Wenbo *et al*. *Environmental Science & Technology*[J], 2012, 46(22): 12 623
39 Wang Min, Liu Qiong, Zhang Yajie *et al*. *Journal of Inorganic Materials*[J], 2013, 28(2): 153 (in Chinese)
40 Gao Fengyu, Tang Xiaolong, Yi Honghong *et al*. *Journal of Central South University: Science and Technology*[J], 2015, 46(6): 2382 (in Chinese)
41 Xiong Lixian, Liu Ting, Wang Jing *et al*. *Journal of Fuel Chemistry and Technology*[J], 2010, 38(1): 85 (in Chinese)

钾盐沉积对VMoTi催化剂脱硝性能的影响

吴彦霞[1]，王献忠[2]，梁海龙[1]，陈　鑫[1]，陈　琛[1]，戴长友[3]，陈玉峰[1]
(1. 中国建筑材料科学研究总院 陶瓷科学研究院，北京 100024)
(2. 萍乡学院 江西省工业陶瓷重点实验室，江西 萍乡 337055)
(3. 瑞泰科技股份有限公司，北京 100024)

摘　要：采用浸渍法（IM）与溶胶凝胶法（Sol-gel）制备VMoTi催化剂，并在实验室模拟选择性催化还原（SCR）催化剂的碱金属K中毒，通过X射线衍射、BET比表面积测试法、NH_3-程序升温脱附（TPD）、H_2-程序升温还原（TPR）和光电子能谱等方法对催化剂表面的理化性能进行分析，并探讨钒钛系催化剂的反应及失活机理。结果表明：与浸渍法制备的VMoTi催化剂相比，溶胶凝胶法制备的VMoTi催化剂具有较小的晶粒粒径，较大的比表面积和孔容，较多的表面酸量，较强的氧化还原能力以及较高的V^{4+}、Mo^{4+}和表面活性氧含量，因此，VMoTi （Sol-gel）催化剂表现出了较好的脱硝效率，在180~320 ℃的温度区间内，脱硝效率稳定在约100%。钾的加入会导致催化剂中毒，且不同方法制备的催化剂的中毒效应不同，K盐沉积对浸渍法制备的VMoTi催化剂的脱硝效率影响较大，溶胶凝胶法制备的VMoTi催化剂具有较好的抗K金属中毒的性能。通过对催化剂的表征发现，K盐削弱了活性成分与载体间的相互结合作用，增强了锐钛矿型TiO_2衍射峰的强度，降低了催化剂表面酸性及氧化还原性，同时催化剂表面的化学吸附氧及V^{4+}、Mo^{4+}等活性金属含量降低，这些因素是造成催化剂活性下降的主要原因。

关键词：催化剂；碱金属；K中毒；失活

作者简介：吴彦霞，女，1988年生，硕士，中国建筑材料科学研究总院陶瓷科学研究院，北京 100024，E-mail：yanxiawu1988@163.com